CHEMISTRY
A EUROPEAN JOURNAL

DOI: 10.1002/chem.200600882

Strategies To Stabilize New Oxides in the $Sr_{n+1}(CoTa)_nO_{3n+1}$ Ruddlesden–Popper Homologous Series

Khalid Boulahya, Marina Parras, and José María González-Calbet*[a]

Abstract: Two new oxides of the Ruddlesden–Popper series have been isolated and structurally characterized in the Sr-Co-Ta-O system. X-ray and electron diffraction and high-resolution electron microscopy show that polycrystalline Sr_3CoTaO_7 constitutes the $n=2$ member of a new $Sr_{n+1}(CoTa)_nO_{3n+1}$ homologous series, the essential feature of which is the existence of two connected Co/Ta octahedral layers, separated by Sr atoms. Sr_2CoTaO_6, the $n=\infty$ member of the series, shows a particular short-range ordering of Co and Ta at the octahedral sites leading, as shown by high-resolution electron microscopy, to the disordered intergrowth of simple and double perovskite type domains. Strategies to stabilize new oxides of this series are discussed.

Keywords: high resolution electron microscopy · layered compounds · perovskite phases · solid-state structures · X-ray diffraction

Introduction

The excellent chemical and thermal stability of perovskite-related oxides combined with their electronic properties make them adequate materials for number of usages dealing with catalysis, energy storage, transport, and conversion as well as information storage and electronics. In particular, cobaltites have been the subject of intensive research due to their enormous ability to adopt different structures leading to promising materials for different applications. For instance, besides the interesting electrical properties of the system $La_{1-x}Sr_xCoO_{3-y}$,[1] giant magnetoresistance has been found in $La_{1-x}(Ba,Sr,Ca)_xCoO_{3-y}$[2] and thermoelectric power properties have been reported for $Ca_3Co_4O_9$.[3] The richness of the physical properties of cobaltites is related to the ability of Co ions to adopt, not only several oxidation states, but also various spin states. This is known in the case of the $LaCoO_3$ perovskite, in which cobalt(III) exhibits spin-state transitions as a function of the temperature.[4]

The ability of the cubic perovskite and the rock salt structures to intergrow in an ordered way along (001) planes with the composition AO leads to layered two-dimensional perovskites that have been widely studied, because of their diverse photocatalytic activity, ionic conductivity, magnetic, dielectric, luminescence, and intercalation properties. The discovery of superconductivity in $La_{2-x}A_xCuO_4$ (A = Ba, Sr)[5] and colossal magnetoresistance in $La_{2-2x}Sr_{1+2x}Mn_2O_7$[6] has increased the search of new intergrowth phases with the general formula $(ABO_3)_nAO$, in which the multiple perovskite layers that are n octahedra thick alternate with single AO rock salt layers. These oxides constitute a homologous family, known as the Ruddlesden–Popper (RP) series with the general formula $A_{n+1}B_nO_{3n+1}$, subsequent to the description of $Sr_3Ti_2O_7$ and $Sr_4Ti_3O_{10}$,[7] even though numerous $n=1$ members of the series were previously described according to the K_2NiF_4 structural type.

Most of the RP phases up to now described contain B cations of the first transition series such as Ti, Ni, Cu, and so forth. Recently, related structures to the $n=2$ member of this series, $Sr_3Co_2O_{7-\delta}$, involving the substitution of Co by other metal transition as Ti or Nb, have been reported.[8] However, very little attention has been paid to later transition series.

In recent years, a broad range of complex oxides that include tantalum were reported to exhibit very high photocatalytic activities for water decomposition. Among various interesting reactions, this photoinduced water decomposition into H_2 and O_2 is potentially one of the most promising means of converting photon energy into chemical energy.[9] Complex tantalates such as $ATaO_3$ (A = Li, Na, K),[10] $Sr_2Ta_2O_7$,[11] and anhydrous or hydrated $A_2SrTa_2O_7$ (A = H, K, Rb)[12] have quite different chemical compositions and crystal structures, but they share a common feature: $[TaO_6]$

[a] Dr. K. Boulahya, Dr. M. Parras, Prof. J. M. González-Calbet
Dpto. de Química Inorgánica
Facultad de Químicas, Universidad Complutense de Madrid
28040 Madrid (Spain)
Fax: (+34) 91-394-4352
E-mail: jgcalbet@quim.ucm.es

octahedra are interconnected along one, two, or three dimensions. The $ATaO_3$ basic structure corresponds to the cubic perovskite formed by a three-dimensional (3D) framework of $[TaO_6]$ corner-sharing octahedra, the alkaline cation being surrounded by twelve oxygen atoms in dodecahedral coordination. $A_2SrTa_2O_7$ is the $n=2$ member of the Ruddlesden–Popper (RP) type layered perovskite (2D). The structure is built up of two cubic perovskite blocks that intergrow with a SrO rock-salt type layer. Full substitution of the A alkaline cation by an alkaline earth metal could lead to structural changes and concomitant changes in the properties of these materials. Evidently, keeping the cationic A:B ratio in the above compounds, the substitution of a monovalent by a divalent cation in the A sublattice must be accompanied by the partial substitution in B of Ta by another metal that stabilizes lower oxidation states. Thus, taking into account the cobalt versatility, and considering the structural similarities between cobaltites and tantalates, we have explored the Sr-Co-Ta-O system. We report in this paper the first successful results in the Sr-Co-Ta-O system corresponding to a Co/Ta=1:1 ratio. Two new phases have been isolated: a 3D-Sr_2CoTaO_6 perovskite type and a 2D-layered Sr_3CoTaO_7 oxide. These results demonstrate the existence of a new Ruddlesden–Popper homologous series of chemical composition $(Sr_{n+1}(Co_{0.5}Ta_{0.5})_nO_{3n+1})$, in which Sr_2CoTaO_6 and Sr_3CoTaO_7 correspond to the $n=\infty$ and $n=2$ members, respectively. X-ray powder diffraction (XRD), selected-area electron diffraction (SAED) and high-resolution electron microscopy (HREM) have been performed to fully determine the structural details of these new compounds.

Results and Discussion

The synthesis pathway of Sr_3CoTaO_7 has been followed by XRPD. After five days annealing, the XRPD pattern can be apparently indexed on the basis of a single $A_3B_2O_7$, $n=2$ RP single phase. It is known that one can have different members of the RP series ranging from $n=1$ to $n=\infty$ (the ABO_3 perovskite structure). However, the disorder in the stacking increases as n increases, so that for high n values the SrO layers appear as extended defects. In fact, the microstructural study by means of HREM shows that the most part of the crystals are constituted by the disordered intergrowth of different members of the RP series. Actually, in the [010] zone image (Figure 1), $n=2$ regions intergrowth with isolated lamellae of the $n=3$, 4, and 5 members of the mentioned series. Isolated fringes aperiodically dispersed within a related matrix in which they are coherently intergrown constitute new examples of Wadsley defects.[13] As several related superstructures have been detected in the same batch one is tempted to attribute its existence to kinetic reasons. Therefore, since larger annealing periods should lead to a long-range ordering, the sample was re-annealed. After seven days at 1100°C, a fully ordered Sr_3CoTaO_7 single phase was isolated as revealed by XRD, SAED, and HREM.

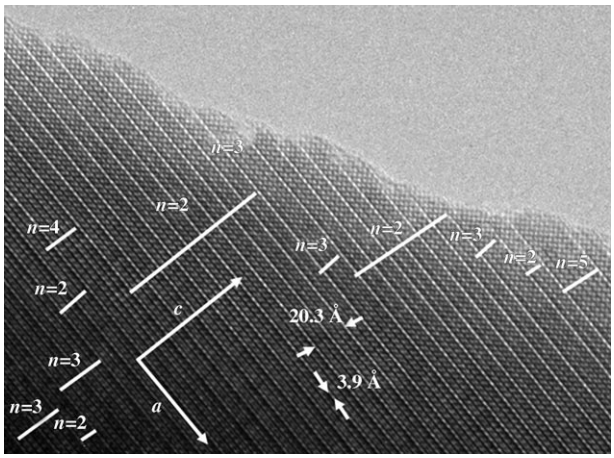

Figure 1. HRTEM image along [010] corresponding to a sample of nominal composition Sr_3CoTaO_7 after five days annealing. Isolated lamellae of $n=3$, 4, and 5 members of $Sr_{n+1}(Co_{0.5}Ta_{0.5})_nO_{3n+1}$ series intergrow, in a disordered way, with $n=2$ regions.

The whole XRPD pattern (Figure 2) can be indexed on the basis of a tetragonal unit cell with lattice parameters $a=b=3.91836(5)$ and $c=20.3226(5)$ Å, with no extra reflections being detected. SAED has been used to fully reconstruct the reciprocal space. The most relevant zone axes, [001] and [010], are depicted in Figure 3. The diffraction spots are always sharp, and no streaking or diffuse intensity, indicative of disordered situations, are observed. All reflections can be indexed in the basis of the above tetragonal unit cell. Besides, the reflection conditions are compatible with the *I*4/*mmm* (139) space group, previously proposed for other $n=2$ members of the RP family.[7]

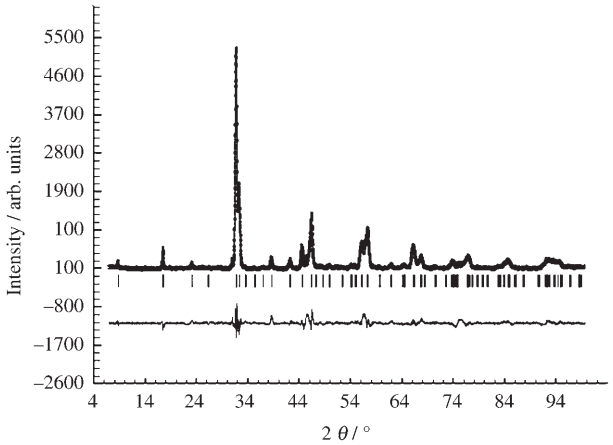

Figure 2. Graphic results of the fitting of the XRD powder data of Sr_3CoTaO_7: experimental (points), calculated (solid line), and difference (bottom).

The [010] HREM image (Figure 4) corresponds to an apparently well-ordered material, showing *d*-spacing of 3.9 and 20.3 Å, corresponding to d_{100} and d_{001}, respectively. The contrast variation in this image corresponds to black dots in a

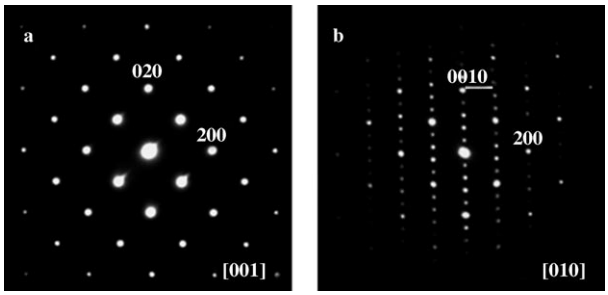

Figure 3. SAED patterns along a) [001] and b) [010] zone axes corresponding to Sr_3CoTaO_7.

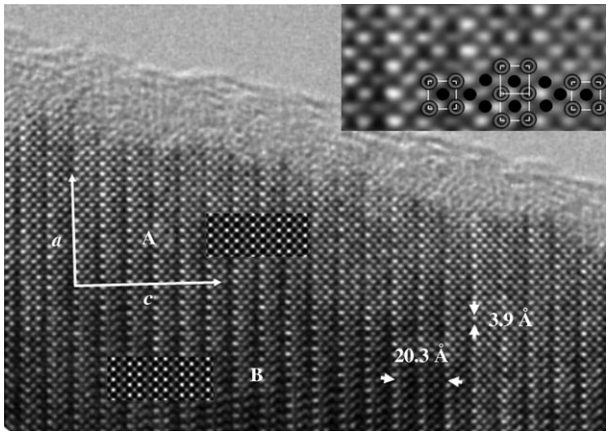

Figure 4. HRTEM image of Sr_3CoTaO_7 along [010]. Enlarged image in which metal atoms are superimposed (black dots correspond to Sr atoms whereas open circles represent Co/Ta atoms). Calculated images are shown in the inset [A ($\Delta t = 30$ Å, $\Delta f = -600$ Å) and B ($\Delta t = 50$ Å, $\Delta f = -500$ Å)].

square configuration displaced by (0.500.5) with respect to the next one, which in turn can be assigned to Co/TaO_6 units; these units are separated by less intense dots corresponding to Sr atoms of the rock-salt blocks. This configuration is shown in the enlarged image of Figure 4 and corresponds to the structural model depicted in Figure 5. Fourier transform was performed on the HREM micrograph, to look for the existence of different domains that could evidence the presence of additional Co/Ta ordering in the structure. However, the whole crystal results homogeneous and no additional ordering was observed. Therefore, from the corresponding ideal atomic coordinates, an image calculation was performed. The simulated image fits nicely with the experimental one (see Figure 4).

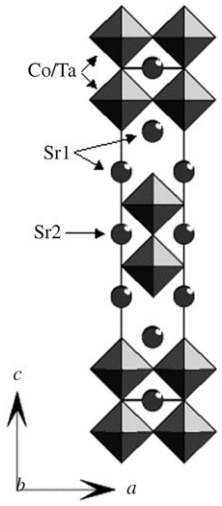

Figure 5. Structural model of Sr_3CoTaO_7 along the *b* axis.

According to the above results, an X-ray profile refinement of Sr_3CoTaO_7 was performed. The structure was solved in the *I*4/*mmm* space group taking the crystallographic data corresponding to an $n = 2$ member of this layered family as starting point.[7] Since no evidence of the presence of Co/Ta order in the B sublattice was detected, both cations were randomly distributed over the octahedral sites in a first stage. Peak shapes were described by pseudo-Voigt functions. Figure 2 shows the graphic results of the fitting of the experimental X-ray diffraction pattern and the difference between observed and calculated data. The refinement was stable and it was possible to refine the positions of oxygen atoms, provided a temperature factor for each type of atom was used. The structure refinement confirms that it is isostructural with $Sr_3Fe_2O_7$.[14] The final structural parameters are collected in Table 1, whereas Table 2 shows some selected interatomic distances.

Table 1. Final structural parameters of Sr_3CoTaO_7.[a]

Atom	*x*/*a*	*y*/*b*	*z*/*c*	U_{iso}	Occ
Sr1	0	0	0.3128(2)	0.71(13)	1.00
Sr2	0	0	0.5	0.71(13)	1.00
T	0	0	0.0967(2)	1.64(14)	0.50
Co	0	0	0.0967(2)	1.64(14)	0.50
O1	0	0.5	0.1052(9)	0.97(12)	1.00
O2	0	0	0.1897(1)	0.97(12)	1.00
O3	0	0	0	0.97(12)	1.00

[a] Space group *I*4/*mmm* (No.139), $a = 3.91836(5)$, $c = 20.3226(5)$ Å, $R_B = 0.047$, $R_{wp} = 0.141$, $R_{exp} = 0.071$, $\chi^2 = 4.1$.

Table 2. Selected interatomic distances [Å] in Sr_3CoTaO_7.

Sr1–O1	2.572(1) × 4	Co/Ta–O1	1.967(2) × 4
Sr1–O2	2.502(4)	Co/Ta–O2	1.890(4)
Sr1–O2	2.771(7) × 4	Co/Ta–O3	1.965(4)
Sr2–O1	2.900(1) × 8		
Sr2–O3	2.771(3) × 4		

The XRD refinement confirms that Sr_3TaCoO_7 constitutes a new example of an $n = 2$ term of the layered RP family. The structure consists of double layers of corner-sharing Co/TaO_6 octahedra running perpendicular to the *c* axis, separated by Sr atoms. Adjacent sets of layers are staggered as shown in Figure 5. The Co/TaO_6 octahedra are slightly distorted, with interatomic Co/Ta–O distances ranging from 1.97(2) to 1.89(2) Å (Table 2). These distances fit well with those of analogous oxides as $K_2SrTa_2O_7$[15] (distances Ta–O, 2.102(1)–1.812(1) Å) or $Sr_3Co_2O_{7-\delta}$[8] in which the Co–O interatomic distances range from 1.92 to 2.00(1) Å. It is noticeable that the Co/Ta–O shortest distance (1.890(4) Å) corresponds to the oxygen O2 atoms unshared at each end of the Co/TaO_6 octahedra. This feature is rather usual and has been also observed in the isostructural $K_2SrTa_2O_7$[15] or in $Sr_4Mn_3O_{10}$[16] (1.77 Å). Finally, the Sr–O (2.84(2)–2.58(4) Å) distances are similar to those observed in other Sr oxides.

As we have previously mentioned, the stabilization of a full ordered Sr_3CoTaO_7 phase is only attained after relatively large annealing periods at 1100 °C. Annealing at higher temperatures does not lead to more ordered situations, but provokes phase decomposition. Actually, Figure 6a shows

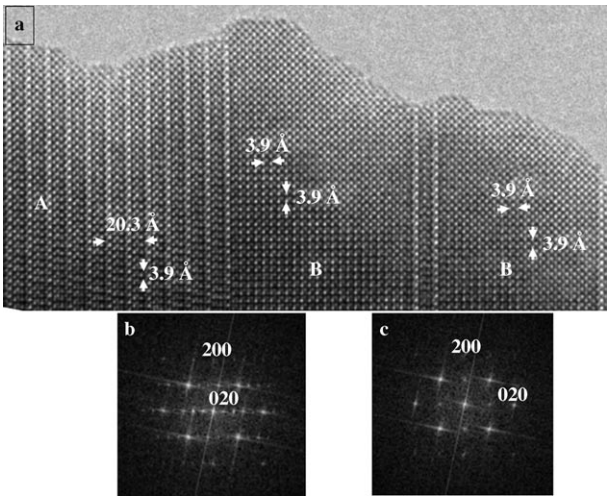

Figure 6. a) HREM image along the [010] zone axis corresponding to a sample of nominal composition Sr_3CoTaO_7 heated at 1200 °C during two days. b) FT corresponding to domains marked A. c) FT corresponding to domains marked B.

the [010] zone image corresponding to a sample of nominal composition Sr_3CoTaO_7 heated at 1200 °C over two days. The presence of two structurally different large domains is evident. The first one, labelled (A), corresponds to the $n=2$ Sr_3CoTaO_7 RP phase, whereas the contrast variation observed in domain B corresponds to a cubic perovskite-type phase. The corresponding FT can actually be indexed on the basis of an $n=2$ tetragonal cell (Figure 6b) and a single perovskite cell (Figure 6c), respectively. The EDS analysis (Figure 7) indicates that cationic ratio changes from Sr/Co/Ta = 3:1:1 in domain A to Sr/Ta/Co = 2:1:1 in domain B, suggesting that a partial lost of Sr occurs at high temperature. This feature is easily understood if we consider that both phases present the same basal plane and only differ along the *c* axis. According to the compositional and structural information provided by EDS and SAED and HREM, a sample with the Sr_2TaCoO_6 composition was prepared. A new stable single phase has been isolated under the thermal conditions indicated in the experimental section.

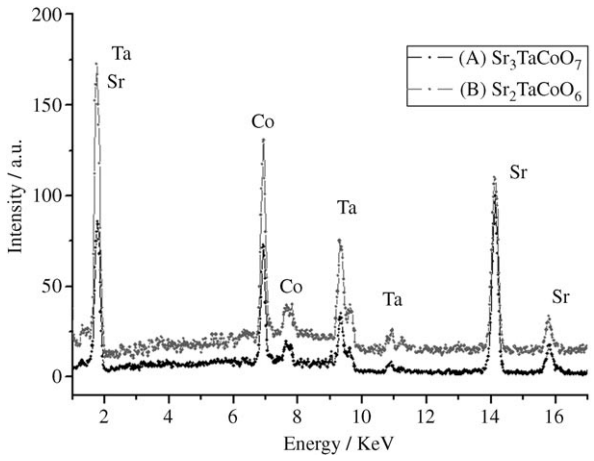

Figure 7. EDS spectra corresponding to zones A and B of the crystal shown in Figure 6.

Sr_2CoTaO_6 was first studied by SAED in order to fully reconstruct the reciprocal space. The most relevant zone axes, [001] [1$\bar{1}$0], and [111] are depicted in Figure 8. Strong reflections correspond to a basic cubic perovskite unit cell. Additional weak spots, as shown by arrows, are observed along the [111] *c* direction and equivalent ones, leading to a double cubic perovskite cell. Actually, all maxima can be indexed on the basis of a double cubic perovskite unit cell with parameter $a=2ac=7.9293(4)$ Å. Besides, the reflection conditions are compatible with the $Fm\bar{3}m$ space group, previously proposed for other double cubic perovskites, such as Ba_2YTaO_6.[17]

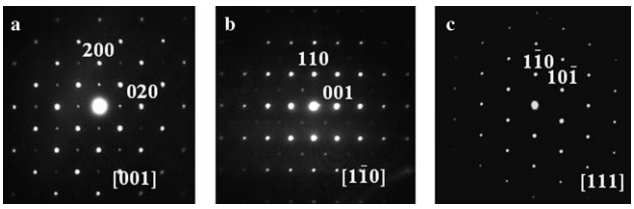

Figure 8. SAED pattern of Sr_2CoTaO_6 along a) [001], b) [1$\bar{1}$0], and c) [111].

On the basis of the above results, an X-ray profile refinement of Sr_2CoTaO_6 was performed. The structure was solved in the $Fm\bar{3}m$ space group taking as starting point the Ba_2YTaO_6 crystallographic data;[17] Co/Ta atoms were randomly distributed through the octahedral sites. Peak shapes were described by pseudo-Voigt functions. Figure 9 shows the graphic results of the fitting of the experimental XRPD pattern and the difference between observed and calculated data. The refinement was stable and it was possible to refine the positions of oxygen atoms, provided a temperature factor for each type of atom was used. The final structural parameters are collected in Table 3. The interatomic distances Co/Ta–O (2.03(2)–1.94(2) Å) and Sr–O (2.84(2) Å) fit well with those of similar oxides also containing corner-sharing octahedra. Figure 10 shows the refined structural model in which two crystallographically different octahedral sites can be distinguished in the average structure. The larger octahedra have 56:44 Ta/Co occupancy whereas the smaller corresponds to the reciprocal ratio. This fact can be explained on the basis of the existence of domains in which a short-range Co/Ta ordering takes place. The structure refinement confirms that it is isostructural with Ba_2YTaO_6, but it is worth stressing that no full order between Co and Ta atoms is observed. For a better understanding of this fact, a

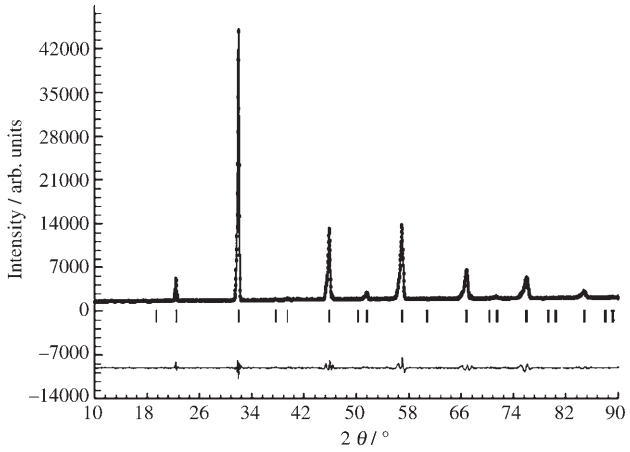

Figure 9. Graphic results of the fitting of the XRD powder data of Sr_2CoTaO_6: experimental (points), calculated (solid line), and difference (bottom).

Table 3. Final structural parameters of Sr_2CoTaO_6.[a]

Atom	*x*/*a*	*y*/*b*	*z*/*c*	U_{iso}	Occ
Sr1	0.25	0.25	0.25	1.10(8)	1.00
Ta/Co1	0	0	0	0.15(6)	0.55/0.45
Ta/Co2	0.5	0.5	0.5	0.15(6)	0.45/0.55
O1	0.744(5)	0	0	1.70(2)	1.00

[a] Space group $Fm\bar{3}m$ (No. 225), $a=7.9280(5)$ Å, $V=498.295(6)$ Å^3. $R_{wp}=0.0496$, $R_{exp}=0.0204$, $R_B=0.0294$, $\chi^2=4.9$.

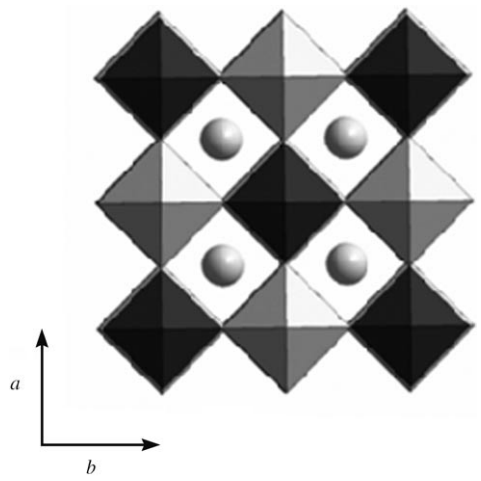

Figure 10. Structural model corresponding to Sr_2CoTaO_6 along the *c* axis.

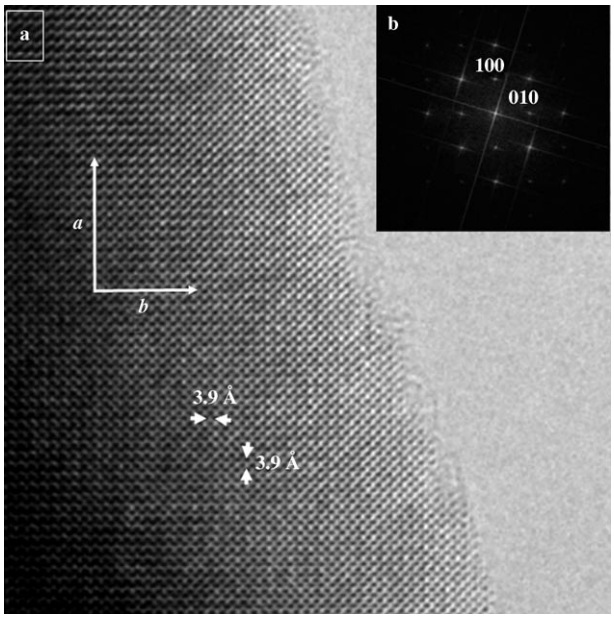

Figure 11. a) HRTEM image of Sr_2CoTaO_6 along [001]; b) corresponding FT.

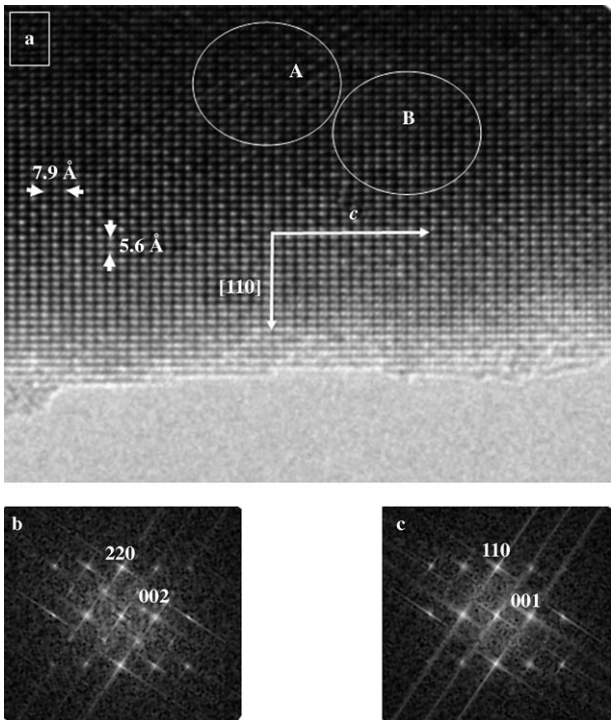

Figure 12. a) HRTEM image of Sr_2CoTaO_6 along $[1\bar{1}0]$; b) FT corresponding to domains marked A; c) FT corresponding to domains marked B.

microstructural study by means of HREM has been performed.

The HREM micrograph along the [001] zone axis (Figure 11a) shows an apparently well-ordered material with *d*-spacing of 3.9 Å, corresponding to d_{100} and d_{010}. Fourier transform was performed on the HREM micrograph, looking for the existence of different domains that could evidence the presence of additional ordering of the structure. However, the whole crystal results homogeneous, only the maxima corresponding to the simple cubic perovskite being observed (Figure 11b). However, the HREM image along $[1\bar{1}0]$ (Figure 12a) reveals the presence of different domains in Sr_2CoTaO_6. Actually, the careful analysis of this micrograph shows the presence of structural domains (outlined by

white circles) corresponding to a double perovskite cell (labeled A) that intergrow in a simple cubic perovskite matrix (B). The optical Fourier transform corresponding to both structural domains are depicted in Figure 12b and c, respectively. These two patterns correspond to the $[\bar{1}10]$ zone axis of a double and a simple cubic perovskite, respectively, and confirm the results obtained by XRPD.

The previously described short-range-order situation is quite usual in ABO_3 perovskite-related oxides in which two different transition metals, with comparable ionic size, occupy the B cationic sublattice. When cationic radii are different enough, a long-range-order configuration is attained and a double perovskite is stabilized. This is the case for Ba_2YTaO_6 ($^{VI}r_Y = 1.04$; $^{VI}r_{Ta} = 0.78$ Å), in which Y and Ta are fully ordered along the B positions.

Conclusion

A new homologous family of the Ruddlesden and Popper series has been described. XRPD, SAED, and HREM have been used to show that Sr_3CoTaO_7 and Sr_2CoTaO_6 constitute the $n=2$ and $n=\infty$ members of the $(Sr)_{n+1}(Co,Ta)_nO_{3n+1}$ homologous series. The first one is formed by two Sr_2CoTaO_6 perovskite blocks which intergrow with one SrO layer, whereas the second one is a double perovskite showing short range ordering of Ca and Ta atoms at the octahedral sites. Electron microscopy observations suggest that, under appropriate synthesis conditions, higher member of the series can be stabilized.

Experimental Section

Polycrystalline samples of Sr_3CoTaO_7 and Sr_2CoTaO_6 were synthesized in platinum crucible by heating stoichiometric amounts of $SrCO_3$ (Aldrich 99.98%), Co_3O_4 (Aldrich 99.9%) and Ta_2O_5 (Aldrich 99+%). Sr_3CoTaO_7 was prepared by heating in air the stoichiometric mixture at 1100 °C for two annealing periods of five and seven days. Sr_2CoTaO_6 was synthesized at 1150 °C for five days. Both samples were quenched to room temperature.

XRPD patterns were collected by using $Cu_{K\alpha}$ radiation ($\lambda = 1.5418$ Å) at room temperature on a PHILIPS X'PERT diffractometer equipped with a graphite monochromator. Diffraction data were analysed by the Rietveld method[18] by using the Fullprof program.[19]

The sample was characterized by SAED and HREM by using a JEOL 3000 FEG electron microscope, fitted with a double tilting goniometer stage (±20°, ±20°). Local composition was analyzed by energy-dispersive X-ray spectroscopy (EDS) with an Oxford analyzer system attached to the above described electron microscope.

Acknowledgements

Financial support by through research projects MAT2004-01248, MAT/0627/2004 and CAM/S-0505/PPQ0316 is acknowledged. K.B. thanks the MCYT (Spain) for financial support under the "Ramón y Cajal" Program.

[1] A. N. Petrov, O. F. Kononchuk, A. V. Andreev, V. A. Cherepanov, P. Kofstad, *Solid State Ionics* **1995**, *80*, 189–199.
[2] G. Briceno, X. D. Xiang, H. Change, X. Sun, and P. G. Schultz, *Science* **1995**, *270*, 273–274.
[3] A. C. Masset, C. Michel, A. Maignan, M. Hervieu, O. Toulemonde, F. Studer, B. Raveau, J. Hejtmanek, *Phys. Rev. B* **2000**, *62*, 166–175.
[4] M. A. Señaris, J. B. Goodenough, *J. Solid State Chem.* **1995**, *118*, 323–336.
[5] J. G. Bednorz, K. A. Müller, *Z. Phys. B* **1986**, *64*, 189–193.
[6] Y. Moritomo, A. Asamitsu, J. Kuwahara, Y. Tokura, *Nature* **1996**, *380*, 141–144.
[7] S. N. Ruddelsden, P. Popper, *Acta Crystallogr.* **1958**, *11*, 54–55.
[8] S. E Dann, M. T. Weller, *J. Solid State Chem.* **1995**, *115*, 499–507.
[9] K. Domen, J. N. Kondo, M. Hara, T. Takata, *Bull. Chem. Soc. Jpn.* **2000**, *73*, 1307–1331.
[10] T. Ishihara, H. Nishiguchi, K. Fukamachi, Y. Takita, *J. Phys. Chem. B* **1999**, *103*, 1–3.
[11] A. Kudo, H. Kato, S. Nakagawa, *J. Phys. Chem. B* **2000**, *104*, 571–575.
[12] K. Shimizu, Y. Tsuji, T. Hatamachi, K. Toda, T. Kodama, M. Sato, Y. Kitayama, *Phys. Chem. Chem. Phys.* **2004**, *6*, 1064–1069.
[13] B. G. Hyde, L. A. Bursill, in *Chemistry of Extended Defects in Non-Metallic Solids* (Eds.: L. Eyring and M. O'Keeffe), North-Holland, Amsterdam, **1970**, pp. 375–378.
[14] E. Lucchini, D. Minichelli, G. Sloccari, *Acta Crystallogr. Sect. B* **1973**, *29*, 2356–2357.
[15] T. A. Kodenkandath, J. B. Wiley, *Mater. Res. Bull.* **2000**, *35*, 1737–1742.
[16] J. Fabry, J. Hybler, Z. Jirak, K. Jurek, K. Maly, M. Nevriva, V. Petricek, *J. Solid State Chem.* **1988**, *73*, 520–523.
[17] M. W. Lufaso, R. B. Macquart, Y. Lee, T. Vogt, H. C. Zur Loye, *Chem. Commun.* **2006**, *14*, 168–170.
[18] H. V. J. Rietveld, *J. Appl. Crystallogr.* **1969**, *2*, 65–71.
[19] J. Rodríguez-Carvajal, *Physica B* **1993**, *192*, 55–69.

Received: June 22, 2006
Published online: October 18, 2006

